# Mobility Management of Multi-hop Mobile Integrated Access and Backhaul Network

Kitaek Lee, Seungwoo Baek, and Saewoong Bahk

***Abstract*—As services and applications utilizing mobile networks grow exponentially, base station (BS) density becomes increasingly dense. There is an increasing demand for wireless backhaul technology for efficient deployment of high-density mobile networks. Although integrated access and backhaul (IAB) technology for efficient operation of wireless backhaul is attracting attention, consideration for mobile IAB (MIAB) is very insufficient. In this work, we propose a novel handover (HO) scheme for MIAB network to reduce handover interruption time (HIT) and radio link failure (RLF) that have a significant impact on users' quality of service (QoS). We investigate HO cases that cover intra-gNB HO, inter-gNB HO, and parent MIAB node HO, and develop their probabilistic models according to the velocities of parent MIAB node and child MIAB node. In addition, we investigate the latency in uplink (UP) control plane (CP) data transmission and each HO case for the baseline MIAB network. Our proposed HO scheme consists of low-latency UL CP data transmission with semi-persistent resource preallocation and RACH-less HO procedure for child MIAB nodes. Through simulation, we verify our proposed MIAB HO scheme outperforms the baseline HO scheme in terms of HO delay and HO overhead.**

***Index Terms*—Handover, integrated access and backhaul (IAB), low-latency handover, mobility management, multi-hop IAB, RACH-less mobility management.**

## I. INTRODUCTION

WITH the development of mobile networks, network services and applications that require high data rates are being developed [1]. Moreover, network services require stable high data rates even in a high mobility environment. For example, users of network service in vehicles want to play high-end games on their smartphones. In addition, autonomous vehicles continuously collect environmental data around the road while driving for safety and driving convenience [2]. This trend will continue in the future, and it is natural that high data rate network services will appear in mobile environments as mobile networks evolve. Therefore, providing seamless high data rates to user devices in mobile environments is an important goal of network system development.

In order to achieve high data rate in 5th generation (5G) mobile networks, studies on the use of wide bandwidth and densification of base stations (BSs) are actively conducted. These efforts appear to use mmWave bands [3] and deploy ultra-dense networks (UDNs) [4]. Leveraging mmWave UDNs improves network performance in urban dense scenarios, but there are challenges to overcome. Radio links using mmWave band are susceptible to high attenuation over distance, so the coverage of mmWave BS is shorter than that of sub-6GHz BS. Despite the wide bandwidth of mmWave band, network performance may be degraded due to the short coverage of mmWave band. Some studies have pointed out impact of frequent handovers (HOs) in mmWave UDN environments [5]–[7]. If HO delays are long and HOs occur too often, which increases network overhead, mmWave UDN cannot provide seamless network service. To improve the performance of next generation mobile network systems, it is necessary to consider the overhead of mobility management.

With the densification of BSs, wireless backhaul technology is attracting attention for cost-effective deployment and flexible operation. The 3rd generation partnership project (3GPP) is actively standardizing integrated access and backhaul (IAB) technologies [8]. In addition, some previous researches have pointed out the benefits of IAB networks in terms of cost effectiveness and flexible network deployment [9]–[11]. IAB technology is one of the key enablers in the post 5G era, and it is expected to further increase network efficiency through deployment flexibility.

Studies on moving cells, so called, mobile BSs are also considered to accelerate the flexibility and effectiveness of wireless backhaul technology [12]. There are previous studies that propose utilizing unmanned aerial vehicles base station (UAV-BS) to provide flexible and traffic-aware BS deployment. Some studies propose that vehicles can be used as BSs [13]. However, taking advantage of mobile BSs requires careful consideration of additional overhead. The mobile BS performs HO when receiving downlink data of a user equipment (UE) via a wireless backhaul link, so the UE cannot receive downlink data during the HO interruption time (HIT) of the mobile BS. Furthermore, quality-of-service (QoS) is much worse when the UE experiences radio link failure (RLF) due to HO of the mobile BS.

In this paper, we propose a low-latency mobility management scheme in mobile IAB (MIAB) multi-hop networks that aims to overcome the short communication range of mmWave band. MIAB nodes contributes to reducing the HO rate compared to the case of using static IAB nodes only, and

Manuscript received May 3, 2022; approved for publication, May 8, 2022. This paper is specially handled by EIC and Division Editor with the help of three anonymous reviewers in a fast manner.

This research was supported in part by the MSIT (Ministry of Science and ICT), Korea, under the ITRC (Information Technology Research Center) support program (IITP-2021-0-02048) supervised by the IITP (Institute of Information & Communications Technology Planning & Evaluation), and in part by the National Research Foundation of Korea (NRF) grant (No. 2020R1A2C2101815 and No. 2022R1A5A1027646).

K. Lee, S. Baek, and S. Bahk are with the Department of ECE and INMC, Seoul National University, Seoul, Korea. email: {ktlee, swbaek}@netlab.snu.ac.kr, sbahk@snu.ac.kr.

S. Bahk is the corresponding author.

Digital Object Identifier: 10.23919/JCN.2022.000018

Creative Commons Attribution-NonCommercial (CC BY-NC).
This is an Open Access article distributed under the terms of Creative Commons Attribution Non-Commercial License (http://creativecommons.org/licenses/by-nc/3.0) which permits unrestricted non-commercial use, distribution, and reproduction in any medium, provided that the original work is properly cited.

1229-2370/22/$10.00 © 2022 KICS

help to decrease network overhead caused by high mobility of users. However, since MIAB nodes have mobility, we should consider other types of mobility of nodes, such as parent MIAB nodes, when calculating HO overhead. In the current multi-hop MIAB network, child MIAB nodes are disconnected when their parent MIAB node performs HO. A child MIAB node is disconnected from its parent MIAB node even if the link quality between the child MIAB node and the parent MIAB node is still best and the child MIAB node still maintains synchronization with the parent MIAB node. Such disconnection causes unnecessary random access, so increases HO latency.

Therefore, we propose a HO scheme that supports the radio resource control (RRC) re-configuration of child MIAB nodes without random access channel (RACH) process when the parent MIAB node performs HO to another gNB. Moreover, we propose an efficient uplink (UL) control plane (CP) data transmission scheme to solve the problem of increased latency for UL data transmission due to the characteristics of multi-hop networks. Through the integration of the proposed HO scheme and UL CP data transmission scheme, we can reduce HO latency even in the multi-hop network architecture.

### A. Contributions

The contributions of the proposed MIAB mobility management scheme can be summarized as follows.

- We investigate the performance of a baseline static IAB (SIAB) network and an MIAB network according to the node mobility, and propose an efficient HO scheme that considers inter-gNB HO of MIAB nodes and inter-gNB HO of parent MIAB nodes.
- We evaluate our proposed scheme and the baseline HO scheme and compare their performance with that of the baseline IAB HO scheme.
- We evaluate the effective spectral efficiency performance of the SIAB and MIAB networks and provide guidelines for using the MIAB network according to the vehicle speed and antenna specifications of the MIAB node.
- To the best of our knowledge, this work is the first that examines the overhead of mobility management and the effectiveness of the HO scheme in multi-hop MIAB networks.

### B. Organization

The rest of this paper is organized as follows. In Section II, we review preliminary studies and related work to understand the MIAB network HO process and its shortcomings. In Section III, we describe the system model of the proposed network. We analyze the overhead of mobility management for the proposed IAB network in Section IV, and provide the proposed low-latency HO scheme for the MIAB network in Section V. We evaluate the performance of the proposed mobility management scheme in Section VI, and conclude this paper in Section VII.

## II. Preliminary Study

In this section, we briefly review previous studies on handover processes, IAB networks, and MIAB networks.

### A. IAB Network and Moving Cells

IAB technology, which can be one of the solutions for efficient deployment and operation of dense network entities in future mobile network systems, is attracting attention. Cudak *et al.* [14] have investigated the advantages of the multi-hop network architecture in the IAB network. The performance of the multi-hop IAB network that shows much higher throughput performance compared to the gNB-only network has been evaluated in [9]. The IAB network performs similarly to the all-wired small cell network in terms of throughput and delay performance. In addition, efforts to improve the performance of the IAB network are continuing in various items such as path selection and resource allocation [15]–[17]. However, previous studies dealing with the IAB network focus on the SIAB network and do not consider the case in which IAB nodes can move.

Studies on moving cells are being actively conducted to maximize the advantages of wireless backhaul link [18], [19]. Moreover, research on the IAB network also highlights the need for the development of MIAB network [20]. Gapeyenko *et al.* [18] propose a novel UAV-BS and cell on wheels BS (COW-BS) [19] based network using mmWave backhaul links. UAV-BS and COW-BS improve network performance in dynamic blockage environments, but mobility management of BSs is not taken into account in those studies. Jaffry *et al.* [19] have conducted a comprehensive study on moving cells. However, they focus on moving cells with passengers in buses or trains, which have the same mobility with mobile BSs.

### B. 5G NR Handover

The handover procedures in 5G NR consist of a handover preparation stage and a handover execution stage. A node that performs HO to a target-gNB (T-gNB) sends a measurement report to its serving-gNB (S-gNB) when a pre-defined measurement event is triggered. The S-gNB sends HO request to the T-gNB and receives HO request ACK from the T-gNB. To indicate that the node can perform HO to the T-gNB, the S-gNB sends RRC connection reconfiguration message with the dedicated random access (RA) preamble ID to the UE. HO execution event starts as the node performs RA to the T-gNB using the dedicated RA preamble. When the RA process is complete, the node sends RRC connection reconfiguration complete message to the T-gNB.

The HO process is terminated when the T-gNB transmits an ACK for the completion of RRC connection reconfiguration, and the node can receive data through the T-gNB. The node cannot receive data in the HO execution stage because it is not connected to any gNB, and the period during which the node cannot receive data is called as the HIT. Since HIT greatly affects users' QoS, reducing HIT is very important in mobility management. Some previous studies have focused on reducing

HIT to enhance performance of mobile networks.

A RACH-less handover scheme is proposed in [21], which removes RACH process incorporating cell radio network temporary identifier (C-RNTI) and timing advance information at RRC connection reconfiguration message. In [6], [22], [23], the authors propose handover skipping techniques to reduce inefficient handover in dense networks. Recent studies focus on efficient handover schemes for high mobility scenarios such as vehicle-to-everything (V2X) and unmanned aerial vehicle (UAV) communications [24], [25]. However, in these studies, only HO according to the mobility of UEs is dealt with, and HO according to the mobility of BSs in a moving cell network is not considered.

### C. Motivation

In a dense network environment, it is important to use the MIAB network that can efficiently improve network performance. Several studies address the need for the MIAB network, but they have not conducted under conditions in which the MIAB network is more favorable than the SIAB network. We investigate the conditions where the MIAB network shows better performance, considering beamforming and mobility management.

However, in the MIAB network, mobility of MIAB nodes causes a performance bottleneck, if there is no consideration for efficient mobility management. The handover process in the multi-hop IAB network causes high latency, and previous studies have not covered this issue in depth. Therefore, we consider the limitations of the baseline HO scheme in the IAB network and propose a way to reduce the delay caused by HO in the multi-hop MIAB network architecture. To the best of our knowledge, the impact of parent IAB node handover on the multi-hop IAB architecture has not been investigated well. This motivates us to focus on mobility management in the multi-hop MIAB network for its efficient utilization.

## III. System Model

### A. Network Model

In this study, we consider a multi-tier mobile IAB network with static gNBs, parent MIAB nodes, child MIAB nodes, and UEs, which is configured in a multi-hop structure. We define static gNBs as IAB donors, each of which consists of a gNB-CU and a gNB-DU. We define parent MIAB nodes and child MIAB nodes as MIAB nodes, each connected to a gNB by 1-hop and 2-hop, respectively. Each UE is 1-hop connected to a child MIAB node. Each parent MIAB node can be assumed to be a special-purpose vehicle to provide network service that is present in a proportion on the road. Child MIAB nodes can be considered private vehicles. A UE can be considered a user's mobile device in a private vehicle (i.e., a child MIAB node). Therefore, the UE is only affected by handovers of the child and parent MIAB nodes since it has the same mobility as the child MIAB node to which it is connected. In addition, since the distance between the UE and the child MIAB node is always kept close at a constant distance, the UE can always be guaranteed good channel state.

We assume that a node with the highest tier (i.e., a gNB) has the largest tx power and beamforming gain, and the lower the tier of the node, the smaller tx power and beamforming gain. We consider a straight two-way road topology where vehicles enter one side and exit the other side. The maximum speeds of parent and child MIAB nodes are denoted by $v_m^{max}$ and $v_c^{max}$, respectively, and we consider a scenario where the maximum speed of child MIAB nodes is greater than that of parent MIAB nodes (i.e., $v_m^{max} \leq v_c^{max}$).

### B. Communication Model

We consider the mmWave channel model in [26].

$$PL(d)[dB] = \alpha + 10\beta \log_{10} d, \tag{1}$$

where $d$ is the distance in meters, $\alpha$ has the values of $61.4$ and $69.8$ for 28 GHz and 73 GHz carrier frequencies, respectively, and $\beta$ is set to 2 for the both frequencies. The downlink received signal power of receiver node $j$ from transmitter node $i$ is defined as

$$P_{i,j}^{rx} = P_i^{tx} - PL(d_{i,j}) + \xi, \tag{2}$$

where $P_i^{tx}$ is the transmit power of node $i$, $d_{i,j}$ is the distance between node $i$ and node $j$, and $\xi$ is a log normal random variable which has $\sigma$ for its standard deviation. We consider a noise-limited mmWave communication model in a 3-D beamforming and outdoor environment where the interference effect is small [27]. The SNR of the received signal can be calculated as $P_{i,j}^{rx}/N_0$.

### C. Directional Beamforming Model

To mitigate high signal attenuation of mmWave band, we consider directional beamforming. We denote the directivity gain of the main beam as $G_b$ and the beamwidth of the main beam as $\theta_b$. We use the directivity gain and the beamwidth model in [28], [29]. Thus, we have

$$G_b = N, \tag{3}$$

where $N$ is the number of antenna array elements. We also have

$$\theta_b = 2 \arcsin(\frac{2}{N}). \tag{4}$$

A tx node (e.g., a gNB or a parent MIAB node) and a rx node (e.g., a parent MIAB node or a child MIAB node) need beam alignment to obtain optimal directivity gain. If a parent MIAB node and its child MIAB node keep a beam pattern too long, the beam drift effect [30] occurs, which can reduce throughput. We define the average effective spectral efficiency (ESE) between node $i$ and node $j$, $ESE_{i,j}$ as

$$ESE_{i,j} = \frac{1}{\tau_b} \int_{\tau_{tr}}^{\tau_b} log_{10} \left(1 + SNR_{i,j}\left(t\right)\right) dt, \tag{5}$$

where $\tau_b$ and $\tau_{tr}$ represent beam training period and beam training duration, respectively. As shown in (5), increasing $\tau_b$ increases average throughput when accurate beam alignment is kept for a long time. However, when $\tau_b$ gets longer, average throughput may decrease in an environment where beam drift frequently occurs. That is, as the relative speed between nodes $i$ and $j$ becomes large, the possibility of beam misalignment increases.

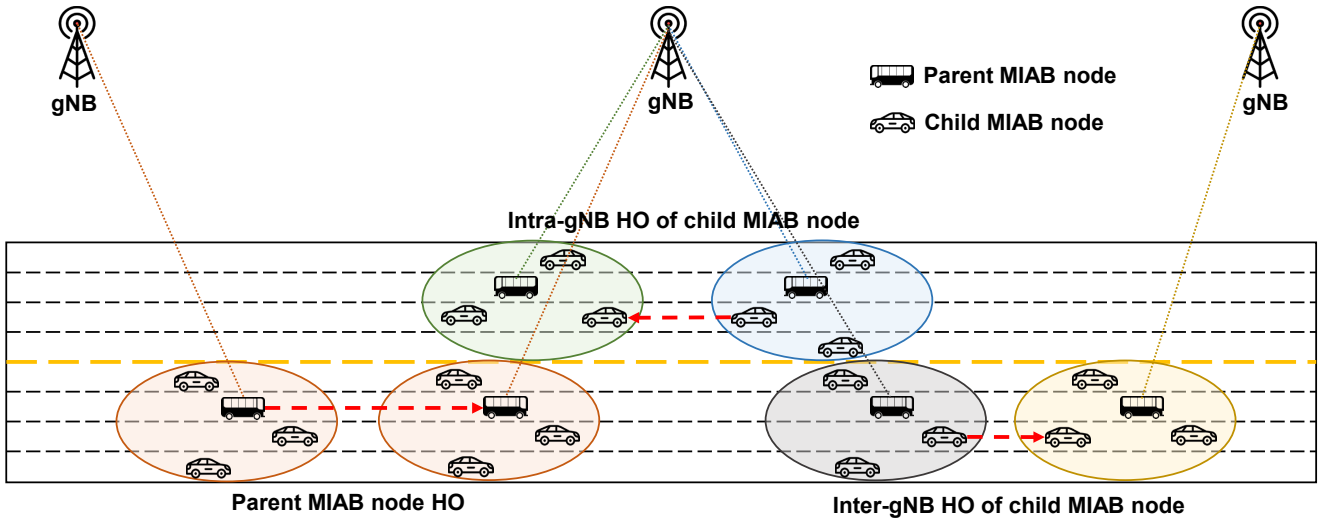


Fig. 1. Handover model in MIAB network.

### D. Handover Model

In the proposed MIAB network model, we define three types of HO: Intra-gNB HO, inter-gNB HO, and parent MIAB node HO, as shown in Fig. 1. Intra-gNB HO is defined as a child MIAB node performing HO to a target parent MIAB node under the same current gNB. Inter-gNB HO is defined as a child MIAB node performing HO to a target parent MIAB node connected to a new gNB. Lastly, parent MIAB node HO to a new gNB occurs due to the mobility of the parent MIAB node, while child MIAB nodes maintain their connection with the same parent MIAB node. The HO process for MIAB node is similar to the current 5G HO process in many ways. A child MIAB node performing HO configures an RRC connection with a T-gNB via a target parent MIAB node starting with RACH preamble transmission to the target parent MIAB node. Control plane (CP) data for RRC configuration should be transmitted to the T-gNB since only gNBs, not MIAB nodes, have RRC layer.

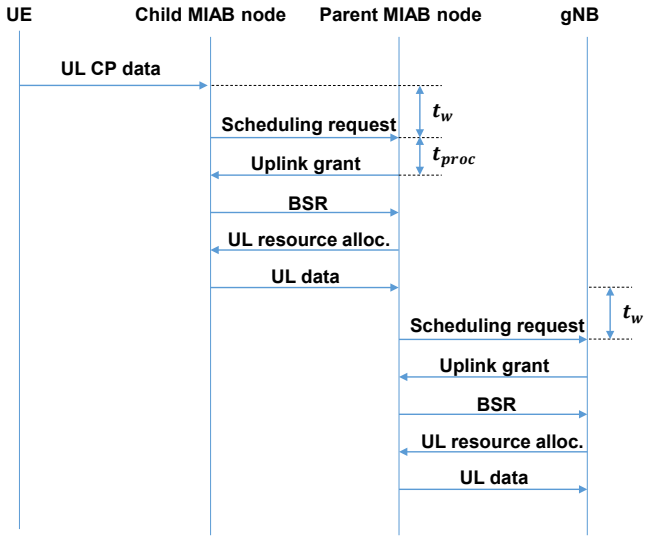


Fig. 2. UL CP transmission latency in the current multi-hop IAB network.

## IV. Analysis of Mobility Management in MIAB Networks

In this section, we investigate the mobility management procedures of multi-hop IAB network and network performance under mobility. First, we analyze latency of UL CP data transmission in multi-hop network architecture. Second, we develop a HO latency model for MIAB node or UE according to the number of hops from the gNB. Finally, we analyze HO probabilities in a dense urban scenario to understand the frequency of HOs according to the types of HOs that occur in the MIAB network.

### A. UL CP Data Transmission Latency

Due to the nature of the multi-hop network architecture, data transmission latency increases as the number of hops increases. In particular, this feature is more pronounced in UL data transmission than in downlink (DL) data transmission. A series of resource allocation processes are required since each node must be allocated UL resource to transmit UL data. A MIAB node can transmit UL data to its parent MIAB node only after UL resource allocation. Due to a series of resource allocation processes, multi-hop network architecture increases UL data transmission latency. For example, a child MIAB node is not directly connected to the gNB, so it may transmit UL CP data through the parent MIAB node. Fig. 2 describes the UL CP data transmission latency in a multi-hop MIAB network. We can define the UL transmission delay from a child MIAB node to its parent MIAB node for UL CP data as

$$t^{c\to p}_{\text{UL, base}} = t^{SR}_{w} + 4t_{proc} + 5t_{tx}, \tag{6}$$

where $t^{SR}_{w}$ is the waiting time for scheduling request, $t_{proc}$ is the node processing delay, and $t_{tx}$ is the transmission delay.

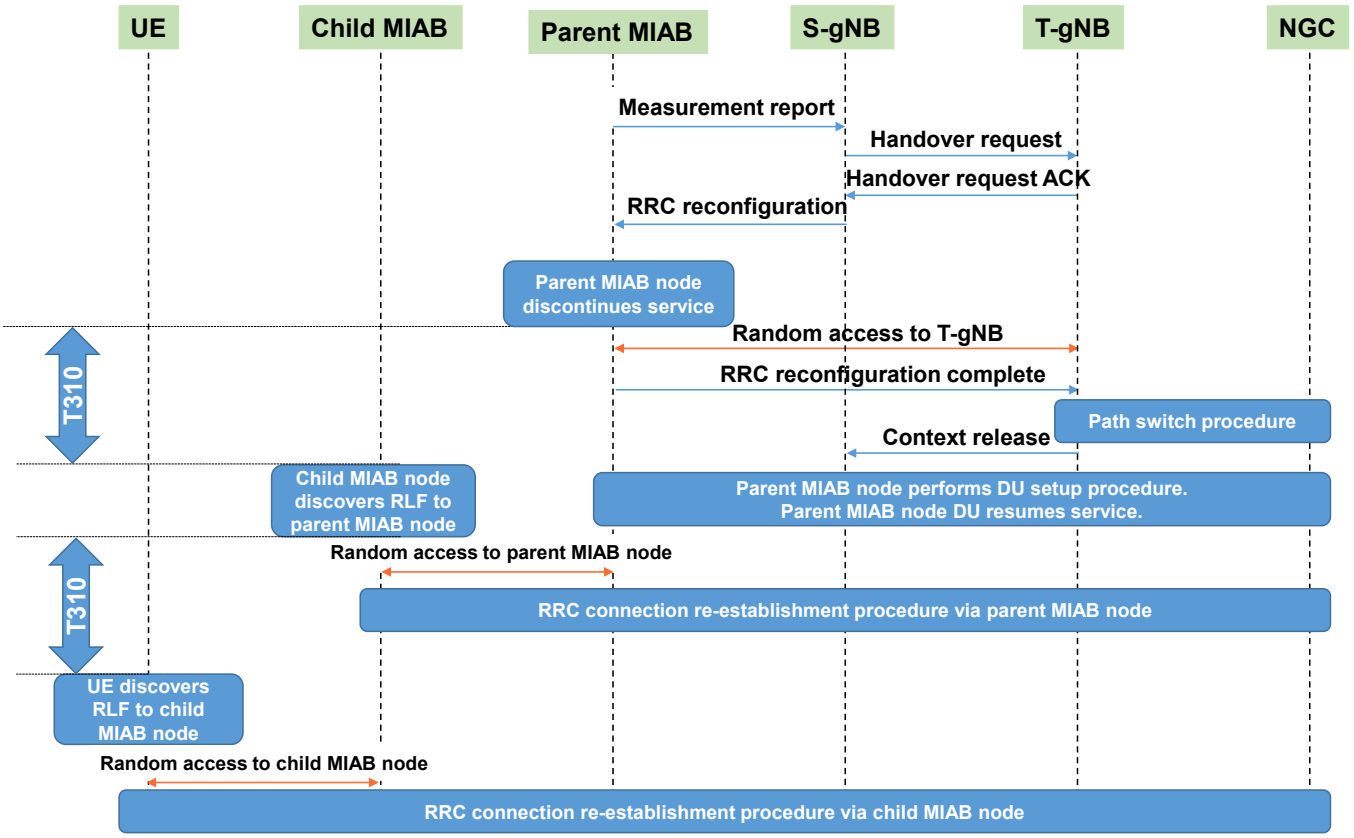


Fig. 3. Baseline parent MIAB node inter-gNB HO scheme in MIAB network.

Likewise, we define the UL CP transmission delay from the parent MIAB node to the gNB as

$$t^{p\to g}_{\text{UL, base}} = t^{c\to p}_{\text{UL, base}} = t^{SR}_{w} + 4t_{proc} + 5t_{tx}. \quad (7)$$

Therefore, we can define the total UL CP transmission delay from the child MIAB node to the gNB as

$$t^{c\to g}_{\text{UL, base}} = t^{c\to p}_{\text{UL, base}} + t^{p\to g}_{\text{UL, base}} = 2t^{SR}_{w} + 8t_{proc} + 10t_{tx}. \quad (8)$$

Fig. 2 depicts the baseline UL CP data transmission procedures from a UE to a gNB. The delay of UL CP data transmission, which is critical to performance of mobility management, becomes very high in baseline HO scheme because the UL scheduling request should be performed for UL transmission of all MIAB nodes.

### *B. Handover Latency*

We analyze HO latency depending on the number of hops from a gNB to a child MIAB node or a UE in the current MIAB mobility management scheme. We divide the HO latency into two types of latency: The HO latency of child MIAB node itself and the HO latency due to the HO of its parent MIAB node. We focus on HIT and RLF duration during which the child MIAB node or the UE cannot receive DL packets.

HIT is defined as the time between when random access to the target node is performed and when the RRC re-establishment process is completed. We calculate the HIT of the parent MIAB node directly connected to the gNB in the same way as the HIT of the mobile node performing HO. However, the HIT of the child MIAB node connected to the gNB by multi-hops increases with the number of hops. We analyze the HO delay when the child MIAB node experiences intra-gNB HO, inter-gNB HO, and parent MIAB node HO, respectively.

The HO delays of the child MIAB node in intra-gNB HO and inter-gNB HO cases are the same. The child MIAB node performs RACH to the target parent MIAB node with $t_{\text{RACH}}$ delay. After the RACH process, the new parent MIAB node transmits RRC message to the gNB through UL scheduling request process with delay of $t^{p\to g}_{\text{UL, base}}$. For the RRC re-establishment process between the gNB and the child MIAB node, DL and UL transmissions are performed in two hops, respectively. Therefore, we can express the HO delay of the child MIAB node as

$$t^{\text{child}}_{intra} = t^{\text{child}}_{inter} = t^{c\to p}_{\text{RACH}} + t^{c\to p}_{\text{UL, base}} + 2t^{p\to g}_{\text{UL, base}} + 2t_{\text{DL}}, \quad (9)$$

where $t_{\text{DL}}$ is the downlink transmission delay, given as

$$t_{\text{DL}} = t_{tx} + t_{proc}. \quad (10)$$

Normally, RLF of the child MIAB node occurs when the signal strength decreases as the distance from the parent MIAB node increases. However, even when the link quality toward the parent MIAB node is still good, the child MIAB node

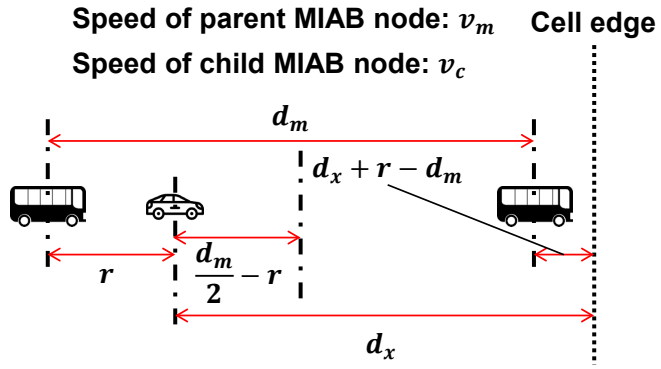


Fig. 4. Topology for the analysis of handover probability.

suffers from RLF when the parent MIAB node discontinues DU operation during the parent MIAB node's HO execution. When the child MIAB node fails to decode N310 number of physical downlink control channels (PDCCHs) of its parent MIAB node consecutively, it starts its T310 timer. The T310 timer expires when the child MIAB node cannot decode N311 number of PDCCHs consecutively. After the child MIAB node discovers RLF (i.e., after the T310 timer expires), it tries RRC re-establishment process via random access. Then we can define the child MIAB node's delay of the parent MIAB node HO as

$$t_{PHO}^{\text{child}} = t_{T310} + t_{\text{RACH}} + 2t_{\text{UL, base}}^{p\to g} + t_{\text{UL, base}}^{c\to p} + 2t_{\text{DL}}, \quad (11)$$

where $t_{T310}$ is the duration of T310 timer.

The HO delay becomes more severe for UEs connected to a child MIAB nodes (e.g., passengers in the vehicle). In the case of the inter-gNB HO of child MIAB node, UEs suffer RLF and should perform RRC connection through three hops. We can describe the UE HO delay caused by the inter-gNB HO of the child MIAB node as

$$t_{inter}^{\text{UE}} = t_{T310} + t_{\text{RACH}} + 2t_{\text{UL, base}}^{p\to g} + 2t_{\text{UL, base}}^{c\to p} + t_{\text{UL, base}}^{u\to c} + 3t_{\text{DL}}. \quad (12)$$

Similarly, when the HO of the parent MIAB node occurs, we calculate the UE HO delay as

$$\begin{aligned} t_{PHO}^{\text{UE}} = {} & 2t_{T310} + t_{\text{RACH}} + 2t_{\text{UL, base}}^{p\to g} \\ & + 2t_{\text{UL, base}}^{c\to p} + t_{\text{UL, base}}^{u\to c} + 3t_{\text{DL}}. \end{aligned} \quad (13)$$

In (11) and (13), since $t_{T310}$ is several hundred ms, the delay in the parent MIAB node HO case is the largest.

### C. Handover Probability

According to (9) and (11), the HO latency of the child MIAB node significantly increases when the parent MIAB node performs inter-gNB HO. We analyze the intra-gNB HO probability of the child MIAB node, the inter-gNB HO probability of the child MIAB node, and inter-gNB HO probability of the parent MIAB node. We investigate the HO probability of each HO type according to the location of the child MIAB node. Fig. 4 shows the road topology indicating the locations of the child MIAB node, the parent MIAB node, and the target parent MIAB node. We denote the distance between the location of the child MIAB node and the boundary point of two gNBs on the road as $d_x$. We assume that the distance between parent and target parent MIAB nodes is constant as $d_m$.

The parent MIAB node is at a distance of $r$ behind the child MIAB node on the road, which is a random variable uniformly distributed between $-d_m/2$ and $d_m/2$. $d_x$ is also a random variable uniformly distributed between 0 and $d_g$, where $d_g$ is the inter site distance (ISD) of gNBs. We consider three types of HO scenarios: Child MIAB node (intra-gNB), child MIAB node (inter-gNB), and parent MIAB node (inter-gNB); they are determined by which MIAB node satisfies the mobility condition first. The conditions to satisfy each HO type are as follows.

- **Child MIAB node (intra-gNB HO):** The child MIAB node arrives at the boundary of two parent MIAB nodes before the target parent MIAB node arrives at the gNB boundary.
- **Child MIAB node (inter-gNB HO):** The child MIAB node arrives at the boundary of two parent MIAB nodes before the parent MIAB node arrives at the gNB boundary, after the target parent MIAB node arrives at the gNB boundary.
- **Parent MIAB node (inter-gNB HO):** The parent MIAB node arrives at the gNB boundary before the child MIAB node arrives at the boundary of two parent MIAB nodes.

In the first case, we can express the condition that the child MIAB node arrives at the boundary of two parent MIAB nodes before the target parent MIAB node arrives at the gNB boundary, as

$$\frac{\frac{d_m}{2} - r}{v_c - v_m} < \frac{d_x + r - d_m}{v_m}, \quad (14)$$

$$r > -\frac{(d_x - d_m)(v_c - v_m)}{v_c} + \frac{v_m d_m}{2v_c}. \quad (15)$$

In the second case, we can write the condition that the child MIAB node arrives at the boundary of two parent MIAB nodes before the parent MIAB node arrives at the gNB boundary and after the target parent MIAB node arrives at the gNB boundary, as

$$\frac{d_x + r - d_m}{v_m} \le \frac{\frac{d_m}{2} - r}{v_c - v_m} \le \frac{d_x + r}{v_m}, \quad (16)$$

$$\begin{aligned} -\frac{d_x(v_c - v_m)}{v_c} + \frac{v_m d_m}{2v_c} \le r \\ \le -\frac{(d_x - d_m)(v_c - v_m)}{v_c} + \frac{v_m d_m}{2v_c}. \end{aligned} \quad (17)$$

Finally, we can express the condition that the parent MIAB node arrives at the gNB boundary before the child MIAB node arrives at the boundary of two parent MIAB nodes, as

$$\frac{\frac{d_m}{2} - r}{v_c - v_m} > \frac{d_x + r}{v_m}, \quad (18)$$

$$-\frac{d_x(v_c - v_m)}{v_c} + \frac{v_m d_m}{2v_c} > r. \quad (19)$$

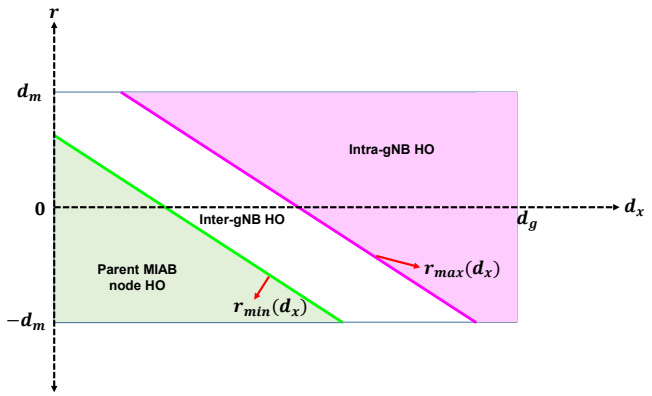


Fig. 5. Illustration of handover probability.

We can obtain Intra-gNB HO probability $p_{intra}(r, d_x)$, inter-gNB HO probability $p_{inter}(r, d_x)$, and parent MIAB node HO probability $p_{PHO}(r, d_x)$, as

$$p_{intra}(r,d_x)=\begin{cases}\frac{1}{d_g d_m}, & \text{if } r_{max}(d_x)<r<\frac{d_m}{2}\\ 0, & \text{otherwise,}\end{cases} \tag{20}$$

$$p_{PHO}(r,d_x)=\begin{cases}\frac{1}{d_g d_m}, & \text{if } -\frac{d_m}{2}<r<r_{min}(d_x)\\ 0, & \text{otherwise.}\end{cases} \tag{21}$$

$$p_{inter}(r,d_x)=\begin{cases}\frac{1}{d_g d_m}, & \text{if } \min(r_{max}(d_x),\frac{d_m}{2})\le r\\ & \quad \le \max(r_{min}(d_x),-\frac{d_m}{2})\\ 0, & \text{otherwise,}\end{cases} \tag{22}$$

where $r_{max}(d_x)=-\frac{(d_x-d_m)(v_c-v_m)}{v_c}+\frac{v_m d_m}{2v_c}$ and $r_{min}(d_x)=-\frac{d_x(v_c-v_m)}{v_c}+\frac{v_m d_m}{2v_c}$. Fig. 5 geometrically shows the three cases of HO to illustrate their probabilities. When the child MIAB node is within $d_x$, we obtain the probabilities of $p_{intra}(d_x)$, $p_{inter}(d_x)$, and $p_{PHO}(d_x)$ as the marginal probability distributions of $p_{intra}(r, d_x)$, $p_{inter}(r, d_x)$, and $p_{PHO}(r, d_x)$, respectively.

$$\begin{aligned}p_{intra}(d_x)&=\int_{-\infty}^{\infty}p_{intra}(r,d_x)\,dr\\&=\frac{\max(\frac{d_m}{2},r_{max}(d_x))-\max(-\frac{d_m}{2},r_{max}(d_x))}{d_m d_g},\end{aligned} \tag{23}$$

$$\begin{aligned}p_{PHO}(d_x)&=\int_{-\infty}^{\infty}p_{PHO}(r,d_x)\,dr\\&=\frac{\min(\frac{d_m}{2},r_{min}(d_x))+\min(-\frac{d_m}{2},r_{min}(d_x))}{d_m d_g},\end{aligned} \tag{24}$$

$$\begin{aligned}p_{inter}(d_x)&=\int_{-\infty}^{\infty}p_{inter}(r,d_x)\,dr\\&=\frac{1}{d_g}-p_{intra}(d_x)-p_{PHO}(d_x).\end{aligned} \tag{25}$$

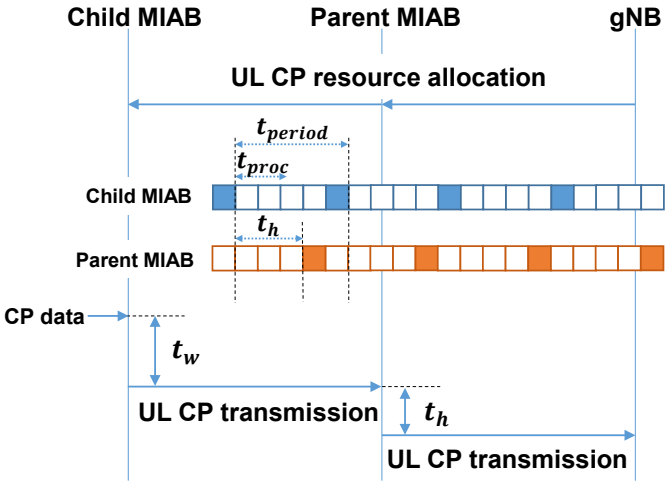


Fig. 6. Proposed UL CP transmission scheme.

Finally, regardless of the child MIAB node's location, we can write $p_{intra}$, $p_{inter}$, and $p_{PHO}$ as

$$\begin{aligned}p_{intra}&=\int_0^{d_g}p_{intra}(d_x)\,dd_x\\&=\frac{1}{2d_m d_g}\Bigg(\left(d_g-\frac{d_m}{2}\right)\\&\quad+\max\left(d_g-\left(\frac{d_m(v_m+v_c)}{2(v_c-v_m)}+d_m\right),0\right)\Bigg)\\&\quad\times\min\left(\frac{d_m}{2}-r_{max}(d_g),d_m\right),\end{aligned} \tag{26}$$

$$\begin{aligned}p_{PHO}&=\int_0^{d_g}p_{PHO}(d_x)\,dd_x\\&=\frac{1}{2d_m d_g}\Bigg(\left(\frac{v_m d_m}{2v_c}+\frac{d_m}{2}\right)\\&\quad+\max\left(\frac{d_m}{2}+r_{min}(d_g),0\right)\Bigg)\\&\quad\times\min\left(\frac{d_m(v_m+v_c)}{2(v_c-v_m)},d_g\right),\end{aligned} \tag{27}$$

$$\begin{aligned}p_{inter}&=\int_0^{d_g}p_{inter}(d_x)\,dd_x\\&=1-p_{intra}-p_{PHO}.\end{aligned} \tag{28}$$

## V. Proposed Mobile IAB Handover Scheme

In this section, we describe the details of the proposed HO scheme for MIAB nodes that consists of two parts: Low-latency UL CP data transmission and parent MIAB node HO maintaining child MIAB nodes' connection.

### A. Low-Latency UL CP Data Transmission Scheme

As shown in the previous section, the latency for transmitting UL CP data becomes long due to the nature of

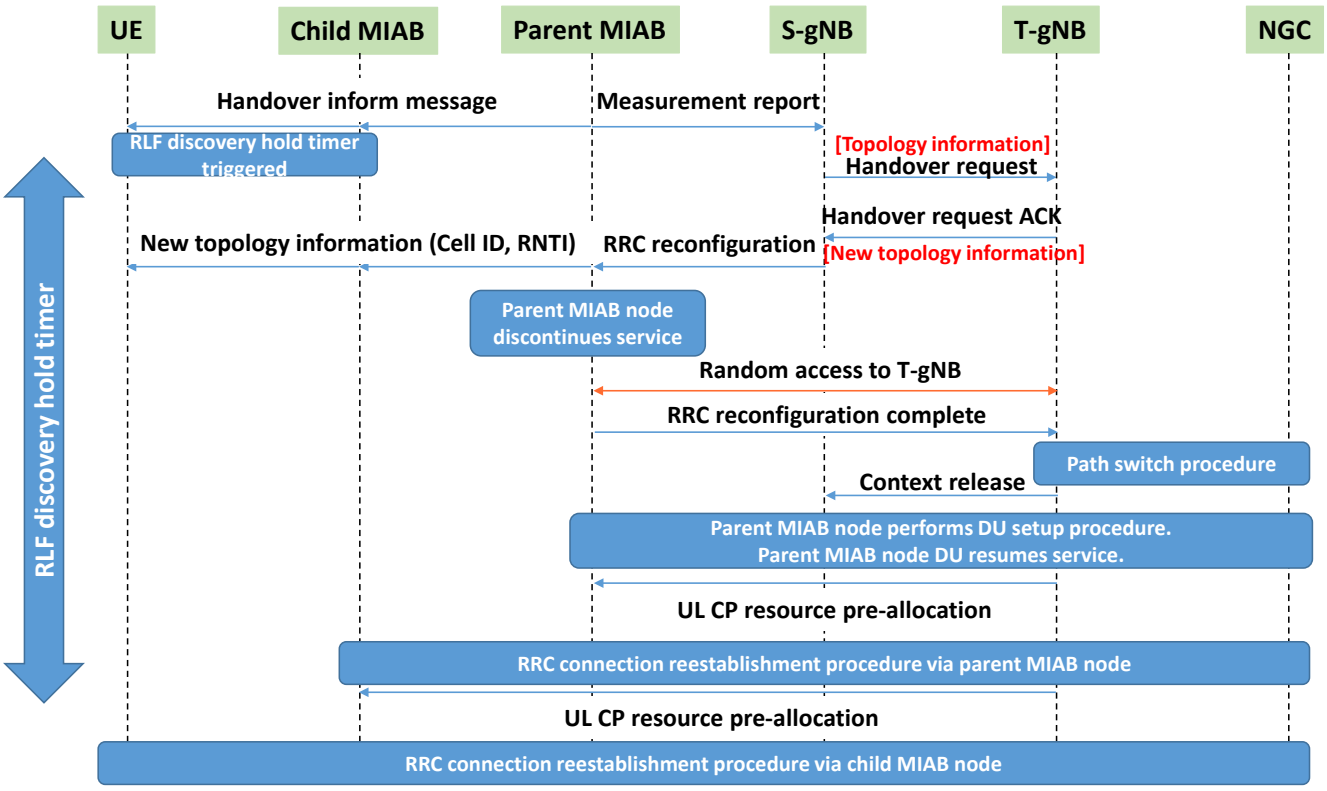


Fig. 7. Proposed parent MIAB node handover scheme for multi-hop MIAB network.

multi-hop network architecture. The increased UL CP data transmission latency gives a great impact on HO performance. This implies, mobile nodes may fail to receive DL data during HIT, decreasing average throughput. Therefore, reducing UL CP data transmission latency has a significant impact on users' QoS improvement.

We propose a UL CP data transmission scheme in multi-hop IAB network without UL resource allocation for every hop using semi-persistent scheduling. The first step in the proposed UL CP transmission scheme is to determine the amount of UL resources to transmit UL CP data. When a gNB notices that UL CP data will be transmitted through multi-hops, the gNB-CU pre-allocates PUCCHs capable of transmitting UL CP data for each hop. As we only consider the HO scenario, the T-gNB pre-allocates PUCCHs after the parent MIAB node performs HO for child MIAB nodes or UEs. The child MIAB nodes that have received UL CP data from the UE already has UL resources for transmitting UL CP data to the parent MIAB node after $t_h$, considering the processing delay (i.e., $t_h > t_{proc}$). When the child MIAB node transmits UL CP data to the parent MIAB node, we can calculate the UL CP data transmission delay as

$$t^{c\to p}_{\text{UL, propose}} = t_w + t_{tx}. \tag{29}$$

Likewise, when the parent MIAB node transmits UL CP data to the gNB, we obtain the UL CP data transmission delay as

$$t^{p\to g}_{\text{UL, propose}} = t_h + t_{tx}. \tag{30}$$

Note that $t_w$ in (29) is changed to $t_h$ in (30). Therefore, the total UL CP data transmission delay from the child MIAB node to the gNB is the sum of (29) and (30):

$$t^{c\to g}_{\text{UL, propose}} = t_w + t_h + 2t_{tx}. \tag{31}$$

Note that (31) is significantly smaller than (8), since the proposed UL CP data transmission scheme removes the delay in the scheduling request procedure. Fig. 6 shows an example that the child MIAB node transmits UL CP data to the gNB. If the child MIAB node should perform random access, we can calculate the total delay as

$$t^{c\to g}_{\text{RACH, propose}} = t_{\text{RACH}} + t^{p\to g}_{\text{UL, propose}}. \tag{32}$$

### *B. Inter-gNB Handover Scheme*

The main drawback of the baseline MIAB node HO scheme is that when a parent MIAB node performs HO, the network connection between the parent and child MIAB nodes is lost. After the parent MIAB node discontinues its DU operation for HO, the child MIAB node cannot receive their PDCCH from the parent MIAB node. The child MIAB node that has not received PDCCH during T310 timer discover RLF, so it should perform RACH again for initial access process. Although the channel state between the parent and child MIAB node is maintainable, the child MIAB node suffers from RLF due to the inter-gNB HO of the parent MIAB node.

The child MIAB node does not need to perform RACH again if it can receive cell ID and RNTI information from the

TABLE I
SIMULATION ENVIRONMENTS

| Parameter | Value |
|---|---|
| ISD of gNBs | 300 m |
| Initial ISD of MIAB nodes | 100 m |
| ISD of SIAB nodes | {50, 100} m |
| Carrier frequency | 28 GHz |
| Subcarrier spacing | 60 kHz |
| Speed of the parent MIAB node | 40–60 km/h |
| Speed of the child MIAB node | 40–100 km/h |
| Pathloss parameters $\alpha$ and $\beta$ | 61.4 and 2 |
| Standard deviation of shadowing | 5.8 |
| gNB tx power | 45 dBm |
| Parent MIAB node tx power | 35 dBm |
| L1 and L3 Measurement period | 40 ms |
| TTT | 240 ms |
| Handover trigger condition | A3 event [31] |
| A3 offset | 3.5 dB |
| Hysteresis | 3 dB |
| RACH period | 10 ms |
| Scheduling request period | 10 ms |
| Transmission delay | 0.25 ms |
| gNB and MIAB node processing delay | 1 ms |

new gNB. This is because synchronization between the child MIAB node and the parent MIAB node is still maintained even if the connection is disconnected due to the HO of the parent MIAB node. Therefore, we propose a novel HO process to guarantee connectivity between the parent and child MIAB nodes when the parent MIAB node performs HO. Fig. 7 shows the proposed MIAB HO process of the parent MIAB node. The first step in the proposed MIAB HO process is to advertise the HO of the parent MIAB node to its child MIAB nodes. Child MIAB nodes that receive HO inform message from the parent MIAB node start the RLF discovery hold timer. Each child MIAB node waits for RRC reconfiguration message from the target gNB-CU during the RLF discovery hold timer. After the parent MIAB node sends HO inform message to child MIAB nodes, the parent MIAB node that performs HO sends a measurement report message to the S-gNB to start the HO process.

The S-gNB sends HO request to the T-gNB, receive HO request ACK, and send RRC connection reconfiguration message to the parent MIAB node. The T-gNB conveys new topology information that contains the cell IDs of the the parent MIAB node and the child MIAB node and RNTIs to all nodes in new topology (the parent MIAB node, the child MIAB node, and the UE). When the HO preparation event ends, the parent MIAB node discontinues DU operation and performs random access to T-gNB. The procedures until the parent MIAB node completes the DU setup are the same as in the baseline HO scheme.

The child MIAB node waits RRC messages from T-gNB via the parent MIAB node with the information of new topology. After the DU setup of the parent MIAB node is completed, the T-gNB sends RRC connection re-establishment message to the child MIAB node and pre-allocates resource for UL CP data transmission. The child MIAB node performs RRC connection with the T-gNB by sending RRC connection re-establishment complete message to the T-gNB. Similarly, the UE performs RRC connection with the T-gNB after receiving

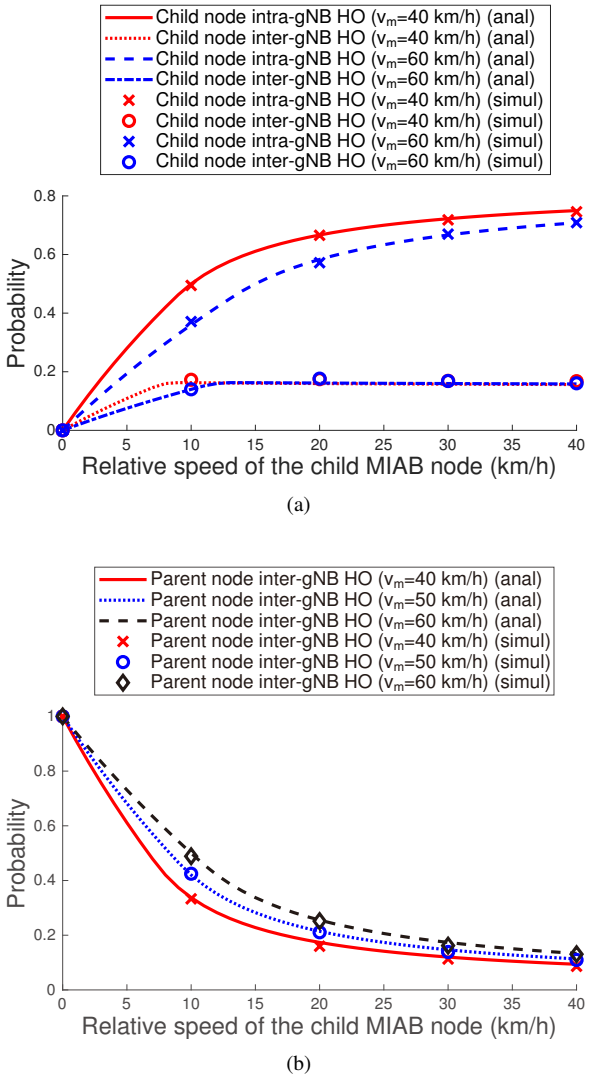


Fig. 8. Expected HO probabilities: (a) Child MIAB node intra-gNB and inter-gNB HO and (b) parent MIAB node inter-gNB HO.

RRC connection re-establishment message via the child MIAB node. The child MIAB nodes and the UE experience reduced HO delay because they do not discover RLF and do not perform unnecessary random access.

The proposed parent MIAB node's inter-gNB HO scheme allows the child MIAB node to have decreased HO delay as

$$t_{PHO}^{child} = t_{\text{RACH}}^{p\to g} + 2t_{\text{DL}} + t_{\text{UL, propose}}^{c\to g}. \quad (33)$$

The inter-gNB and intra-gNB HO delays are given as

$$t_{intra}^{\text{child}} = t_{inter}^{\text{child}} = t_{\text{RACH}}^{c\to p} + t_{\text{UL, propose}}^{p\to g} + t_{\text{UL, propose}}^{c\to g} + 2t_{\text{DL}}. \quad (34)$$

The HO delay in the inter-gNB and intra-gNB HO cases is reduced as the UL CP transmission delay of (9) is reduced to the UL CP transmission delay of (34). Interestingly, the parent MIAB node HO delay of (33) is less than the intra-gNB and inter-gNB HO delay of (34), since the child MIAB nodes do not need to perform random access when the parent MIAB node performs HO in the proposed HO scheme.

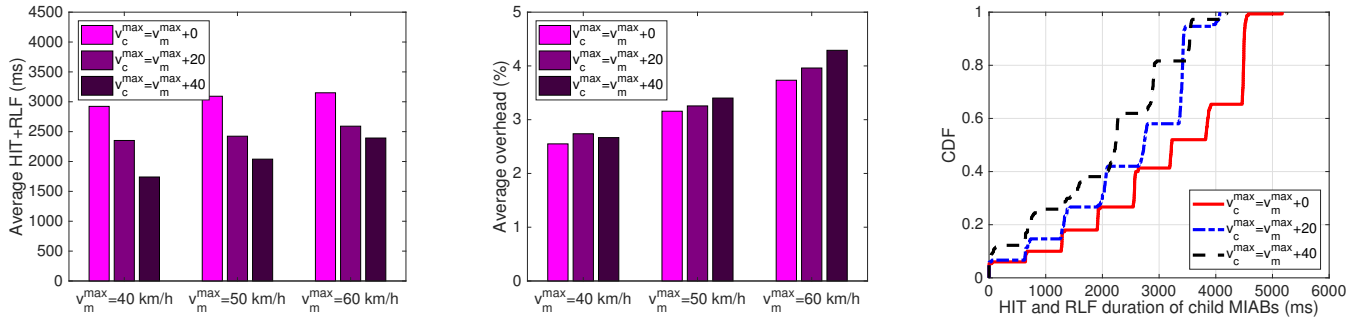


(a) (b) (c)

Fig. 9. Latency and overhead performance of the baseline HO scheme: (a) Average latency, (b) average overhead, and (c) CDF of latency.

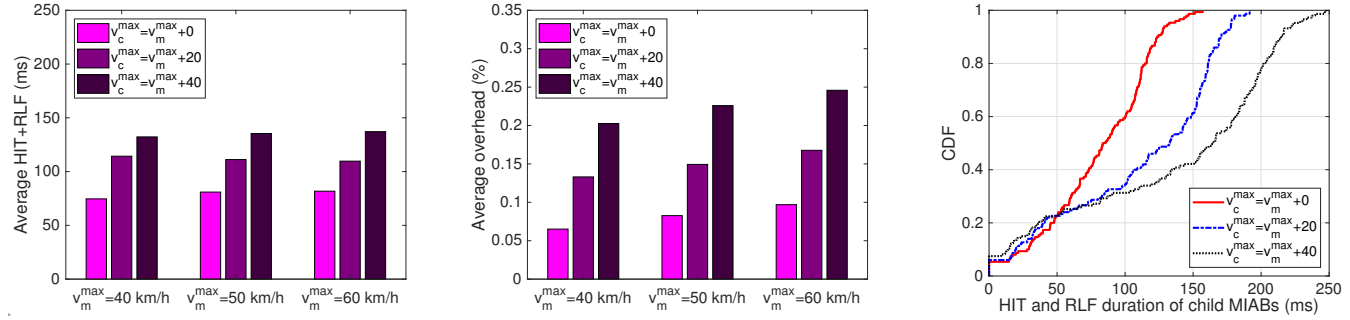


(a) (b) (c)

Fig. 10. Latency and overhead performance of the proposed HO scheme: (a) Average latency, (b) average overhead, and (c) CDF of latency.

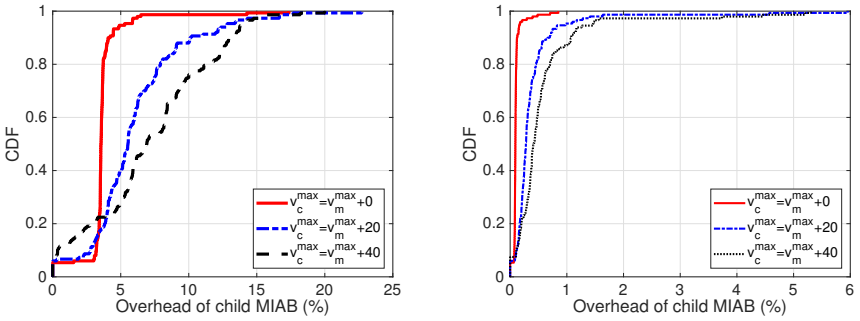


(a) (b)

Fig. 11. CDF of the average HO overhead: (a) Baseline HO scheme and (b) proposed HO scheme.

## VI. Performance Evaluation

In this section, we evaluate the performance of the proposed HO scheme for MIAB network via simulation. We use simulation of urban mobility (SUMO) [32]. The road topology for the simulation is a 1 km long straight two-way road with four lanes in each direction. Since we consider mmWave band, the subcarrier spacing is set to 60 kHz, so the transmission delay is 0.25 ms. We set the maximum speed of the parent MIAB node as 40, 50, and 60 km/h, and the maximum speed of the child MIAB node as 40, 50, 60, 70, 80, 90, and 100 km/h. Note that we only set the maximum speed of the MIAB node and vary its speed depending on traffic conditions. We set the initial ISD of the parent MIAB node as 100 m. After the initial state, ISD is subject to change according to traffic conditions and mobility of MIAB nodes. In addition, we set the RACH period and the scheduling request period as 10 ms. Parameters used in the simulation are shown in Table I.

### A. HO Probability

We validate the probability model for the three HO scenarios analyzed in Section IV. Fig. 8 shows the probabilities of intra-gNB HO of child MIAB node, inter-gNB HO of child MIAB node, and parent MIAB node HO. We calculate each probability according to the speed of the parent MIAB node and the speed of the child MIAB node. In Fig. 8(a), the intra-gNB HO probabilities increase as the relative speed

between the child MIAB node and the parent MIAB node increases. Interestingly, the probability of inter-gNB HO is hardly affected by the speed of the child MIAB node and the parent MIAB node when the speed is above a certain point.

In Fig. 8(b), the probability of the parent MIAB node HO decreases as the relative speed increases. If both MIAB nodes have the same speed, the probability of the parent MIAB node HO is 1. The reason is that inter-gNB HO and intra-gNB HO do not occur since the connection between the child MIAB node and the parent MIAB node is maintained when the speed of the parent MIAB node and the child MIAB node are the same.

### *B. Handover Latency*

We comparatively evaluate the HO delay and overhead performance of the proposed MIAB HO scheme and the baseline HO scheme. The HO delay is the total delay caused by HO experienced by the child MIAB node. That is, HO delay is the sum of HIT and RLF caused by intra-gNB HO, inter-gNB HO, and parent MIAB node HO. Fig. 9 shows the HO latency and overhead results of the baseline HO scheme. Fig. 9(a) shows that the average HO delay increases as the speed of MIAB nodes increases when the relative speed between the child MIAB node and the parent MIAB node is high. If the speed of MIAB nodes and their relative speed are high, the intra-gNB HO probability decreases and the parent MIAB node HO probability increases compared to when the MIAB node speed is low with the same relative speed. As the relative speed gets lower, the HO delay increases because only the parent MIAB node HO with the largest delay occurs.

We define the HO overhead of the child MIAB node as the ratio of HO delay to sojourn time. In other words, the HO overhead is the ratio of the time that the child MIAB node has not received DL data due to mobility management to the time maintaining the topology of the child MIAB node (i.e., no change of routing path from the gNB to the child MIAB node). Fig. 9(b) shows the overhead performance of the baseline HO scheme. Interestingly, the average HO delay has the largest value but the overhead has the smallest value when the relative speed is 0. This is because the intra-gNB HO and the inter-gNB HO frequently occur when the relative speed increases, resulting in reduced sojourn time and increased overhead. In the worst case, the average overhead is up to $4.29\%$ which greatly degrades network performance. On the other hand, as the cumulative distribution function (CDF) in Fig. 9(c) shows, when the relative speed is large, the child MIAB node experiences lower overall delay. However, the total HO delay of the child MIAB node becomes more than 5 s in the worst case.

Fig. 10 shows the performance of the proposed MIAB HO scheme. The overall HO delay is reduced to less than one-tenth of the baseline HO scheme. Different from the baseline HO scheme, the average delay increases when the relative speed is high. This is because the child MIAB node in the proposed HO scheme does not suffer RLF and does not perform RACH even when the parent MIAB node HO occurs, so there is no significant HO delay difference between the parent MIAB node HO and the inter-gNB HO.

As Fig. 10(b) shows, the proposed HO scheme has a very low average overhead of $0.25\%$ even when the average overhead is the highest. The CDF in Fig. 10(c) shows that the HO delay of the child MIAB node increases overall when the relative speed is high. In the proposed HO scheme, the difference in HO delay between intra-gNB HO, inter-gNB HO, and parent MIAB node HO is not significantly different, so the HO delay depends entirely on the frequency of the HO event. That is, since HO occurs frequently when the relative speed is high, the overall HO delay increases. Even so, the HO delay of the worst case child MIAB node in the proposed HO scheme is reduced to 1/20 compared to the child MIAB node in the baseline HO scheme.

Fig. 11 shows the CDF of HO overhead. The HO overhead of the worst case child MIAB node is 22.7% in the baseline HO scheme, and the HO overhead of the worst case of child MIAB node is 5.96% in the proposed HO scheme. Moreover, more than 90% of child MIAB nodes have 1% or less overhead in the proposed HO scheme. This implies that mobility management is performed efficiently in the proposed HO scheme.

### *C. Effective Spectral Efficiency*

The effective spectral efficiency (ESE) considers the beam training overhead and HO overhead. Figs. 12 and 13 show the spectral efficiency results of SIAB and MIAB networks. The number of antenna array elements in Figs. 12 and 13 is set to 32 and 128, respectively. For 32 and 128 antenna array elements, the beamwidths of the main lobe are calculated as $7.17^\circ$ and $1.79^\circ$, respectively, using (4). We set the ISD of parent MIAB nodes to 100 m and the ISD of SIAB nodes to 50 m and 100 m. Fig. 12 shows the spectral efficiency results when wider beams are used with the beam training periods of 40 ms, 80 ms, and 160 ms. When IAB nodes use wider beams, the SIAB network shows better spectral efficiency performance compared with the MIAB network when the ISD of SIAB nodes is 50 m.

However, when IAB nodes use narrow beams which provide higher beamforming gain, the MIAB network outperforms the SIAB network as shown in Fig. 13 even when the ISD of SIAB nodes is closer than the ISD of parent MIAB nodes. Moreover, Figs. 12(c) and 13(c) show the SIAB network cannot support long beam training periods. Otherwise the MIAB network improves the spectral efficiency performance with a long beam training period.

In order to distinguish which network performs better, SIAB network or MIAB network, according to the road environment and the specifications of IAB nodes, we provide the ESE performance with the best combination of the beam training period and the number of antenna elements, as shown in Fig. 14. The maximum number of antenna array elements in Figs. 14(a) and 14(b) are 32 and 128, respectively. The results show that the SIAB network always uses only wide beams, since the ESE performance degrades due to beam drift when using narrow beams. Otherwise, the MIAB network can adaptively select the best combination of beamwidth and beam

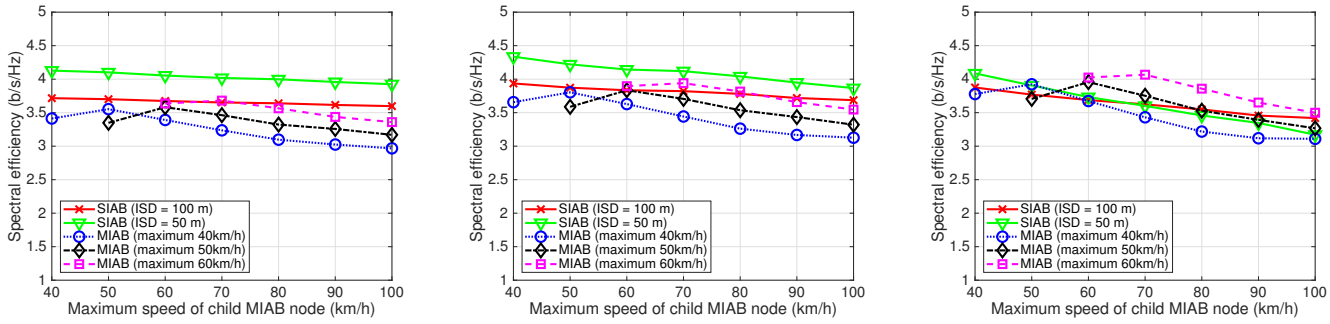


(a) (b) (c)

Fig. 12. Spectral efficiency performance of SIAB network and MIAB network ($N = 32$): (a) $\tau_b = 40$ ms, (a) $\tau_b = 80$ ms, and (c) $\tau_b = 160$ ms.

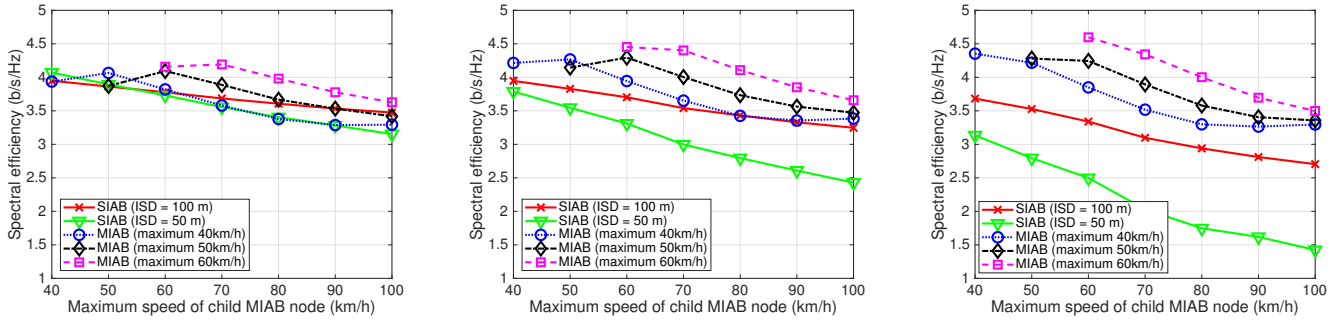


(a) (b) (c)

Fig. 13. Spectral efficiency performance of SIAB network and MIAB network ($N = 128$): (a) $\tau_b = 40$ ms, (a) $\tau_b = 80$ ms, and (c) $\tau_b = 160$ ms.

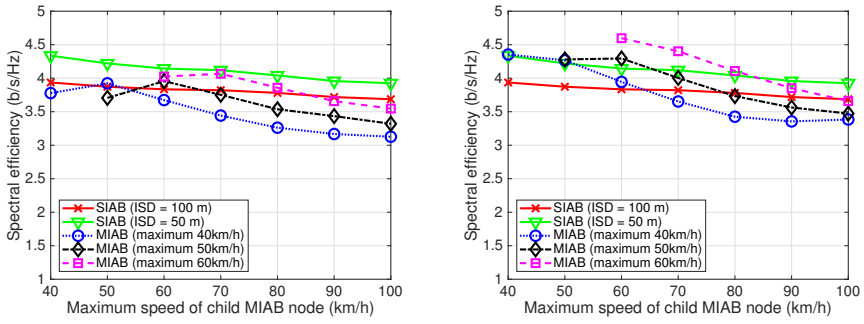


(a) (b)

Fig. 14. Spectral efficiency performance of SIAB network and MIAB network with the best combination of $N$ and $\tau_b$: (a) Maximum number of antenna array elements = 32 and (b) maximum number of antenna array elements = 128.

training period which performs best.

The results show that the MIAB network is generally more advantageous than the SIAB network when IAB nodes can use narrow beams. When the ISD between IAB nodes is equal to 100 m, if we select appropriate speeds for parent MIAB nodes, the MIAB network always shows better performance than the SIAB network, as shown in Fig. 14(b). The MIAB network shows the ESE performance gain of up to 20.09% compared to the SIAB network when the ISDs of MIAB network and SIAB network are the same. Moreover, when the maximum speed of child MIAB nodes is 60 km/h, the MIAB network shows a performance improvement of 11.83% compared to the SIAB network with the ISD of 50 m. The results means that if a large number of antenna arrays can be used, the MIAB network performs better even if the density of IAB nodes is reduced by half compared to the SIAB network. With these results, as shown in Fig. 14, we can decide which network to be chosen between the SIAB network and the MIAB network according to the road condition (i.e., the maximum speed of vehicles) and the antenna specifications of IAB nodes. These results help to deploy an IAB network considering the road condition and the deployment cost.

## VII. Conclusion

In this work, we propose a novel HO scheme for MIAB network to reduce HIT and RLF that greatly affect users'

QoS. We develop the latency model of the baseline mobility management scheme in MIAB network, and the probabilistic models for three HO types: Intra-gNB HO, inter-gNB HO, and parent MIAB node HO according to the velocities of parent and child MIAB nodes. We propose a novel low-latency HO scheme for MIAB network that consists of low-latency UL CP data transmission and parent MIAB node HO. Through extensive simulation, we confirm that the proposed MIAB HO scheme outperforms the baseline HO scheme in terms of HO delay and overhead. In addition, simulation results show that the proposed MIAB network improves the ESE performance compared to the SIAB network. As future work, we will investigate generalized latency models and HO probabilities in terms of hop count in multi-hop MIAB architecture. Moreover, we plan to develop a scheme to adaptively operate the MIAB network in real-world scenarios, taking into account vehicle density and traffic conditions.

## REFERENCES


[1] E.-K. Hong *et al.,* "6G R&D vision: Requirements and candidate technologies," *J. Commun. Netw.,* vol. 24, no. 2, Apr. 2022.

[2] Y. Wang, K. Venugopal, A. F. Molisch, and R. W. Heath, "Blockage and coverage analysis with mmwave cross street bss near urban intersections," in *Proc. IEEE ICC*, 2017.

[3] Y. Niu, Y. Li, D. Jin, L. Su, and A. V. Vasilakos, "A survey of millimeter wave communications (mmwave) for 5G: Opportunities and challenges," *Wireless Netw.*, vol. 21, no. 8, pp. 2657–2676, Apr. 2015.

[4] M. Kamel, W. Hamouda, and A. Youssef, "Ultra-dense networks: A survey," *IEEE Commun. Surveys Tuts.*, vol. 18, no. 4, pp. 2522–2545, May 2016.

[5] E. Demarchou, C. Psomas, and I. Krikdis, "Mobility management in ultra-dense networks: Handover skipping techniques," *IEEE Access*, vol. 6, pp. 11921–11930, Feb. 2018.

[6] R. Arshad, H. ElSawy, S. Sorour, T. Y. Al-Naffouri, and M.-S. Alouini, "Handover management in 5G and beyond: A topology aware skipping approach," *IEEE Access*, vol. 4, pp. 9073–9081, Dec. 2016.

[7] R. Arshad, H. Elsawy, S. Sorour, T. Y. Al-Naffouri, and M.-S. Alouini, "Cooperative handover management in dense cellular networks," in *IEEE GLOBECOM*, 2016, pp. 1–6.

[8] 3GPP, "Study on integrated access and backhaul," 3rd Generation Partnership Project (3GPP), Technical Report (TR) 38.874, Oct. 2018, version 16.0.0.

[9] M. Polese *et al.*, "Integrated access and backhaul in 5G mmwave networks: Potential and challenges," *IEEE Commun. Mag.*, vol. 58, no. 3, pp. 62–68, Mar. 2020.

[10] M. N. Islam, N. Abedini, G. Hampel, S. Subramanian, and J. Li, "Investigation of performance in integrated access and backhaul networks," in *IEEE INFOCOM WKSHPS*, 2018, pp. 597–602.

[11] Y. Zhang, M. A. Kishk, and M.-S. Alouini, "A survey on integrated access and backhaul networks," *arXiv preprint arXiv:2101.01286*, 2021.

[12] S. Andreev, V. Petrov, M. Dohler, and H. Yanikomeroglu, "Future of ultra-dense networks beyond 5G: Harnessing heterogeneous moving cells," *IEEE Commun. Mag.*, vol. 57, no. 6, pp. 86–92, 2019.

[13] J. Heo, B. Kang, J. Yang, J. Paek, and S. Bahk, "Performance-cost tradeoff of using mobile roadside units for V2X communication," *IEEE Trans. Veh. Technol.,* vol. 68, no. 9, Sep. 2019.

[14] M. Cudak, A. Ghosh, A. Ghosh, and J. Andrews, "Integrated access and backhaul: A key enabler for 5G millimeter-wave deployments," *IEEE Commun. Mag.*, vol. 59, no. 4, pp. 88–94, May 2021.

[15] C. Saha, M. Afshang, and H. S. Dhillon, "Bandwidth partitioning and downlink analysis in millimeter wave integrated access and backhaul for 5G," *IEEE Trans. Wireless Commun.*, vol. 17, no. 12, pp. 8195–8210, 2018.

[16] M. Polese, M. Giordani, A. Roy, D. Castor, and M. Zorzi, "Distributed path selection strategies for integrated access and backhaul at mmwaves," in *Proc. IEEE GLOBECOM*, 2018, pp. 1–7.

[17] J. Y. Lai, W.-H. Wu, and Y. T. Su, "Resource allocation and node placement in multi-hop heterogeneous integrated-access-and-backhaul networks," *IEEE Access*, vol. 8, pp. 122937–122958, Oct. 2020.

[18] M. Gapeyenko, V. Petrov, D. Moltchanov, S. Andreev, N. Himayat, and Y. Koucheryavy, "Flexible and reliable UAV-assisted backhaul operation in 5G mmwave cellular networks," *IEEE J. Sel. Areas Commun.*, vol. 36, no. 11, pp. 2486–2496, Oct. 2018.

[19] S. Jaffry, R. Hussain, X. Gui, and S. F. Hasan, "A comprehensive survey on moving networks," *IEEE Commun. Surveys Tuts.*, Oct. 2020.

[20] C. Madapatha *et al.*, "On integrated access and backhaul networks: Current status and potentials," *IEEE Open J. Commun. Society*, vol. 1, pp. 1374–1389, Sep. 2020.

[21] J. Choi and D. Shin, "Generalized rach-less handover for seamless mobility in 5G and beyond mobile networks," *IEEE Wireless Commun. Lett.*, vol. 8, no. 4, Aug. 2017.

[22] R. Arshad, H. ElSawy, S. Sorour, T. Y. Al-Naffouri, and M.-S. Alouini, "Velocity-aware handover management in two-tier cellular networks," *IEEE Trans. Wireless Commun.*, vol. 16, no. 3, pp. 1851–1867, Jan. 2017.

[23] M. Tayyab, X. Gelabert, and R. Jäntti, "A survey on handover management: From LTE to NR," *IEEE Access*, vol. 7, pp. 118907–118930, Aug. 2019.

[24] D. O. Rodrigues, T. Braun, G. Maia, and L. Villas, "Towards sdn-enabled rach-less make-before-break handover in c-v2x scenarios," in *Proc. IEEE WiMob*, 2021, pp. 337–344.

[25] V. Sharma, F. Song, I. You, and H.-C. Chao, "Efficient management and fast handovers in software defined wireless networks using UAVs," *IEEE Netw.*, vol. 31, no. 6, pp. 78–85, Nov. 2017.

[26] M. R. Akdeniz *et al.*, "Millimeter wave channel modeling and cellular capacity evaluation," *IEEE J. Sel. Areas Commun.*, vol. 32, no. 6, pp. 1164–1179, Jun. 2014.

[27] J. G. Andrews *et al.*, "Modeling and analyzing millimeter wave cellular systems," *IEEE Trans. Commun.*, vol. 65, no. 1, pp. 403–430, Jan. 2016.

[28] W. Yi, Y. Liu, A. Nallanathan, and M. Elkashlan, "Clustered millimeter-wave networks with non-orthogonal multiple access," *IEEE Trans. Commun.*, vol. 67, no. 6, pp. 4350–4364, Jun. 2019.

[29] X. Yu, J. Zhang, M. Haenggi, and K. B. Letaief, "Coverage analysis for millimeter wave networks: The impact of directional antenna arrays," *IEEE J. Sel. Areas Commun.*, vol. 35, no. 7, pp. 1498–1512, Jul. 2017.

[30] J. Zhang and C. Masouros, "Beam drift in millimeter wave links: Beamwidth tradeoffs and learning based optimization," *IEEE Trans. Commun.*, vol. 69, no. 10, pp. 6661–6674, Oct. 2021.

[31] 3GPP, "Radio resource control (RRC); protocol specification," 3rd Generation Partnership Project (3GPP), Technical Report (TR) 38.874, Oct. 2018, version 16.0.0.

[32] P. A. Lope *et al.*, "Microscopic traffic simulation using sumo," in *Proc. IEEE ITSC*, 2018, pp. 2575–2582.


**Kitaek Lee** (Graduate Student Member, IEEE) received the B.S. degree in Electrical and Computer Engineering from Seoul National University in 2015. He is currently pursuing the Ph.D. degree with the Department of Electrical and Computer Engineering from Seoul National University. His current research interests are in 5G and 6G wireless communication network systems, mobility management for mobile communication systems, and emerging technologies of next-generation cellular systems.

**Seungwoo Baek** (Graduate Student Member, IEEE) received a B.S. degree in the field of Computer Science from Republic of Korea Air Force Academy in 2011. He is currently pursuing the Ph.D. degree with the School of Electrical and Computer Engineering from Seoul National University. His research interests include the area of public safety communication systems, ad-hoc networks, and next-generation mobile technologies.

**Saewoong Bahk** (Senior Member, IEEE) received the B.S. and M.S. degrees in Electrical Engineering from Seoul National University (SNU), in 1984 and 1986, respectively, and the Ph.D. degree from the University of Pennsylvania, in 1991. He was with AT&T Bell Laboratories as a Member of Technical Staff from 1991 to 1994, where he had worked on network management. From 2009 to 2011, he served as Director of the Institute of New Media and Communications. He is currently a Professor at SNU. He has been leading many industrial projects on 5G/6G and IoT connectivity supported by Korean industry. He has published more than 300 technical articles and holds more than 100 patents. He is a member of the National Academy of Engineering of Korea (NAEK). He was a recipient of the KICS Haedong Scholar Award, in 2012. He was President of the Korean Institute of Communications and Information Sciences (KICS) in 2020. He served as Chief Information Officer (CIO) of SNU from 2016 through 2021. He was General Chair of the IEEE WCNC 2020 (Wireless Communication and Networking Conference), IEEE ICCE 2020 (International Conference on Communications and Electronics), and IEEE DySPAN 2018 (Dynamic Spectrum Access and Networks). He was Director of the Asia–Pacific Region of the IEEE ComSoc. He is an Editor of the IEEE Network Magazine and IEEE Transactions on Vehicular Technology. He was TPC Chair of the IEEE VTC-Spring 2014, and General Chair of JCCI 2015, Co-Editor-in-Chief of the Journal of Communications and Networks (JCN), and on the Editorial Board of Computer Networks Journal and the IEEE Tran. on Wireless Communications.